Numerical Studies of Torus Bifurcations

Article · January 1984

DOI: 10.1007/978-3-0348-6256-1_19

1 author:

William Finlay Langford
University of Guelph

International Series of
Numerical Mathematics, Vol. 70

NUMERICAL STUDIES OF TORUS BIFURCATIONS

W.F. Langford

The normal form equations for the interactions of a Hopf bifurcation and a hysteresis bifurcation of stationary states can give rise to an axisymmetric attracting invariant torus. Nonaxisymmetric perturbations are found to produce phase locking, period doubling, bistability, and a family of strange attractors.

1. Introduction

The major unresolved problem of bifurcation theory today may well be that of understanding the transition to turbulence. This problem has been the subject of several recent books and conferences, see [1-4]. The so-called "main sequence" [5,6] of bifurcations leading to turbulence begins with one or more bifurcations of stationary states, followed by a Hopf bifurcation to a periodic orbit, then a Naimark-Sacker torus bifurcation (and possibly a period doubling cascade), and finally the appearance of a strange attractor representing turbulent flow. Such sequences of transitions have been observed in experiments having simple geometries, for example Rayleigh-Bénard convection [7], Taylor vortices [8], and oscillating chemical reactions [9]. Mathematically, the first two or three bifurcations in this sequence are fairly well understood, and even explain some of the experimental data, but from the torus bifurcation onward very little is understood.

Recent studies of certain vector fields close to a singularity with eigenvalues $\{0,+i\omega,-i\omega\}$ have revealed the existence in this context of the following bifurcation sequence: stationary bifurcation, Hopf bifurcation, bifurcation to an invariant torus; see [10-20]. It is convenient to think of these singularities as resulting from the coalescence of two "primary" bifurcations: a Hopf bifurcation (corresponding to the eigenvalues $+i\omega,-i\omega$) and a bifurcation of stationary states (corresponding to the eigenvalue 0). Then it is not surprising to find stationary and Hopf bifurcations on unfolding the singularity, however the appearance of an invariant torus was unexpected. Its existence is guaranteed in a small open region of the unfolding-parameter space when certain inequalities involving the low order nonlinear terms are satisfied. The primary bifurcation of stationary states entering into this coalescence may be any from a growing list of cases: saddlenode [12], transcritical [10], pitchfork [11,13], hysteresis or cusp [17], and isola. Which case is to be expected in a given problem depends on the number of parameters in the problem and on the presence or absence of symmetries.

This paper is a continuation of the work in the previous paragraph, in that it presents studies of bifurcations that occur after the first appearance of an invariant torus. The approach is numerical, in contrast to the analytical results referenced above. The bifurcations in question involve global dynamics, so complex that analytical techniques are inadequate to give a fully detailed description. One quite recent analytical result, established for the transcritical-Hopf case, is that in a neighborhood of the singular point the relative measure of parameter values corresponding to quasiperiodic flow on the torus approaches unity as the neighborhood shrinks to zero [18]. Another is the observation that, if as the torus grows it approaches a heteroclinic saddle connection, then a theorem of Silnikov may imply the presence of Smale's horseshoes and hence chaotic dynamics [12]. Between these two extremes, very little is known analytically. The present numerical studies help fill this gap and may point the way for future theoretical work. Numerically we find strange attractors with large basins of attraction, in contrast to the "leaky" chaos of the Silnikov mechanism.

2. The Model Equations

The numerical results presented here are for the case of interactions of hysteresis and Hopf bifurcations, a case which is very rich in structure and is still under investigation, but which promises to have important applications. We will assume that the spectrum contains the simple eigenvalues $\{0, +i\omega, -i\omega\}$ with the remainder in the negative half-plane, and that a two-step preliminary transformation of the system has been performed, consisting of first a reduction to the 3-dimensional center manifold, and then a transformation of this system to its Poincaré-Birkhoff normal form. The resulting equations can be written:

$$
\begin{aligned}
x' &= (z - \beta)x - \omega y + \text{h.o.t.} \\
y' &= \omega x + (z - \beta)y + \text{h.o.t.} \qquad (1)\\
z' &= \lambda + \alpha z + az^3 + b(x^2 + y^2) + \text{h.o.t.}
\end{aligned}
$$

Here λ is the bifurcation parameter, and α, β are unfolding parameters, all near 0. The frequency ω comes from the original pure imaginary eigenvalue $i\omega$. The a and b terms are "resonant", and "h.o.t." stands for higher order terms, which do not affect the classification of stationary and periodic solutions, but do influence the full dynamics and especially the flow on and near the torus. In principle, the higher order terms can be transformed to be axisymmetric about the Z-axis up to arbitrarily high order, but the procedure does not converge in general; the neighborhood of validity shrinks to zero as the order is increased. Furthermore, axisymmetry is a highly nongeneric condition. Therefore it seems essential that nonaxisymmetry be retained if the conclusions are to have any practical applications.

The model equations used for numerical investigation were chosen for computational economy while retaining the essential features of (1). The variables and parameters were assumed rescaled to make the leading terms in (1) of order one, then a and b were assigned values -(1/3) and -1 respectively corresponding to one of the most interesting cases in the general classification. The remaining resonant cubic term in the z′ equation was retained along with a simple nonaxisymmetric fourth degree monomial to incorporate important nonaxisymmetric effects. Higher order terms in the x′ and y′ equations have been dropped for the results presented here, their presence does not seem to given bifurcation phenomena qualitatively different from what has been found for (2).

$$
\begin{aligned}
x' &= (z - \beta)x - \omega y \\
y' &= \omega x + (z - \beta)y \qquad (2)\\
z' &= \lambda + \alpha z - z^3/3 - (x^2 + y^2)(1 + \rho z) + \varepsilon z x^3
\end{aligned}
$$

Here ρ and ε are "small", ρ determines the location of the Naimark-Sacker torus bifurcation, and ε controls the nonaxisymmetry. Analogous model equations have been derived from normal forms for the transcritical-Hopf and pitchfork-Hopf cases, and are described in [19,20] and [11,17] respectively.

3. Numerical Results

Since it is the qualitative behaviour of solutions that is of interest, the results are presented here in graphical form. The computations were performed on an IBM personal computer, working in compiled BASIC in double precision with an 8087 numerical coprocessor, and the graphics were produced on a Hewlett-Packard 7470A Plotter. The accuracy of the computations is considered to be sufficient to show the location and qualitative features of attracting sets (ω-limit sets), however the flow inside a strange attractor is characterized by divergence of trajectories and sensitive dependence on intial conditions, so that the numerical solutions do not accurately predict the location of a point on a trajectory inside a strange attractor over long time intervals. Similarly the initial-value methods used here (Runge-Kutta and predictor-corrector) are inadequate for computing unstable orbits of saddle type.

Figures 1 to 13 show a series of computed solutions of system (2) with parameter values $\alpha = 1$, $\beta = 0.7$, $\lambda = 0.6$, $\omega = 3.5$, and $\rho = 0.25$ all held fixed, while the axisymmetry-breaking parameter ε was slowly increased. Each figure shows a single trajectory, plotted as a solid line for $X>0$ and a broken line for $X<0$, after initial transients have died away. For each figure there is a large basin of attraction within which different choices of initial point all lead to the same attractor. Previous studies of (1) and analogous systems have traced the succession of bifurcations leading up to an invariant torus [17,19], so we begin here with the axisymmetric invariant torus in Figure 1. In Figure 2 with $\varepsilon = 0.025$, one sees that the trajectory has become more concentrated in one band around the torus and is less concentrated in an adjacent band. This may be interpreted as a weak resonant interaction between the two oscillations on the torus. As ε increases, there appears to be a saddlenode bifurcation of periodic orbits

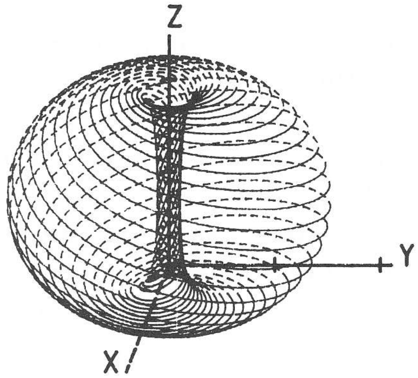

Fig. 1. Torus. Eps=0.0

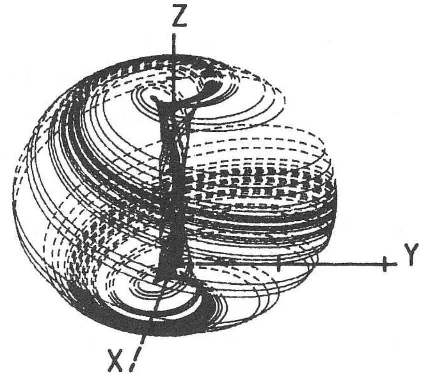

Fig. 2. Torus. Eps=0.025

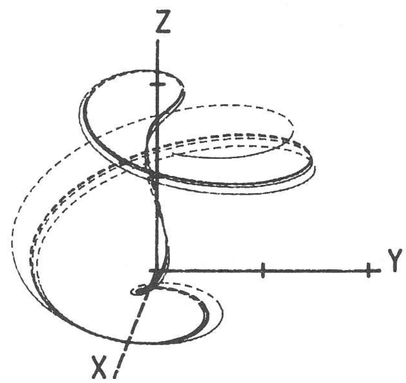

Fig. 3. Period 4. Eps=0.04

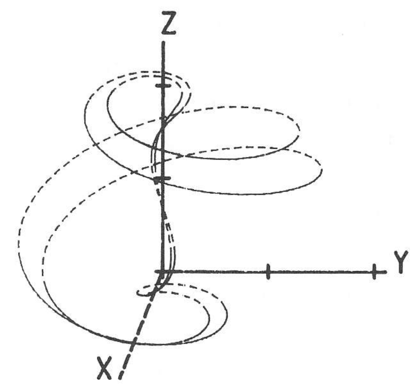

Fig. 4. Period 8. Eps=0.06

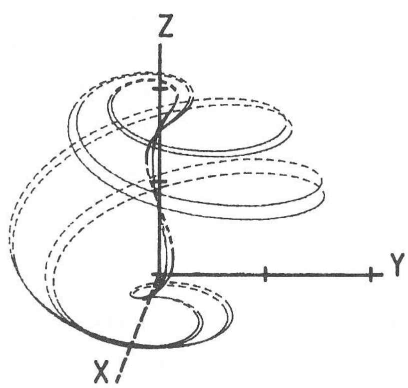

Fig. 5. Period 16. Eps=0.0675

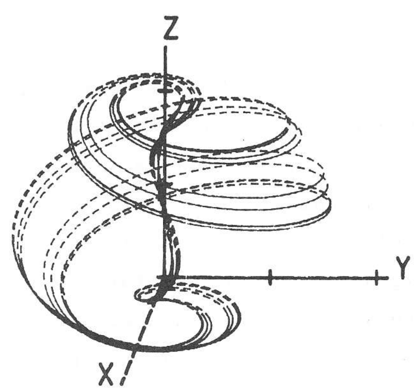

Fig. 6. Period 32. Eps=0.07

within the torus, giving rise to a stable limit cycle and an (unobserved) unstable cycle. Figure 3 shows the period 4 limit cycle observed for $\varepsilon = 0.04$, together with an initial transient portion of a typical solution trajectory. We say that the system is now phase-locked, because the period 4 cycle is preserved if we vary the "forcing" frequency ω over a small interval; from the point of view of dynamical systems theory, the system in Figure 3 is structurally stable. Increasing ε to 0.06 gives the new attractor in Figure 4, a cycle of period 8. The period 4 cycle evidently still exists (between the two loops of the 8-cycle) but is now unstable, and a period-doubling bifurcation has occurred between $\varepsilon = 0.04$ and $\varepsilon = 0.06$. In the process, the smooth toroidal manifold of Figures 1 and 2 has been destroyed, because now a small section containing the period 4 and 8 cycles is folded on itself by 180^0 every four revolutions, rather like a Mobius band. Further increases of ε produce a period doubling cascade, with bifurcation values of ε spaced more and more closely, see Figure 5 for period 16 with $\varepsilon = 0.0675$, and Figure 6 for period 32 with $\varepsilon = 0.07$. We have not tried to compute the Feigenbaum constant for this cascade, however see [21].

Beyond this period doubling cascade, the solutions become even more complicated. For $\varepsilon = 0.09$ there appears to be a "chaotic band" of period 4, see Figure 7. Solutions from initial points in a large basin approach this band quickly, but within the band the motion is aperiodic and effectively unpredictable over long time intervals. Figure 8 shows the same chaotic band in cross-section, cut by the X=0 plane. Figure 8 extends over a much longer time interval than Figure 7; the trajectory (after transients) has intersected the X=0 plane 1000 times (500 Poincaré maps), always falling in one of eight "islands" (four for the Poincaré map) which resemble segments of a curve. The trajectory moves among the islands in the sequence indicated by the numbers 1 to 4 in Figure 8. Note that in this sequence the island undergoes àn S-folding, then the "S" is flattened vertically onto itself and stretched horizontally, and finally it is mapped onto the original island 1. In this process the central portion of the island reverses orientation, i.e. the outside becomes the inside, and the two ends are folded inward. If the attractor is the limit of this sequence as $t \to \infty$ then it can not be simply the short curve segment which it appears to be at

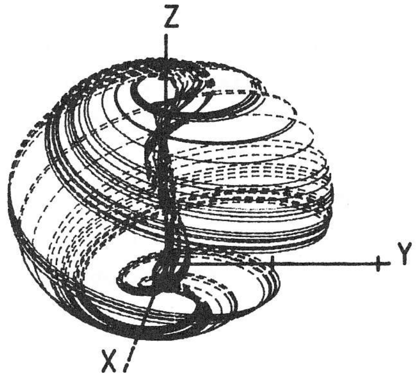

Fig. 7. Chaotic Band. 0.09

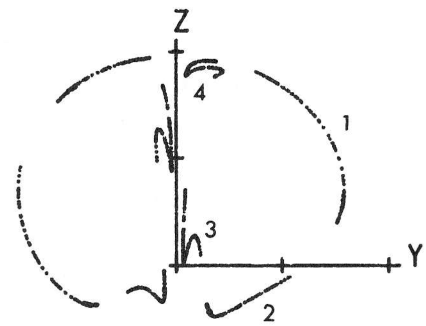

Fig. 8. 500 Poincaré Maps.

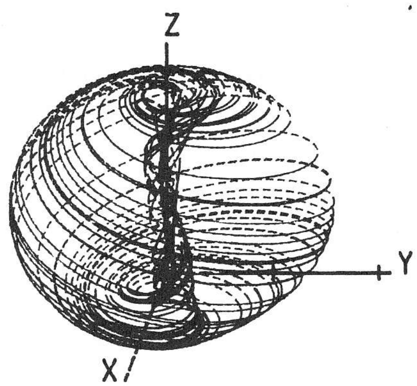

Fig. 9. Folded Torus. 0.1

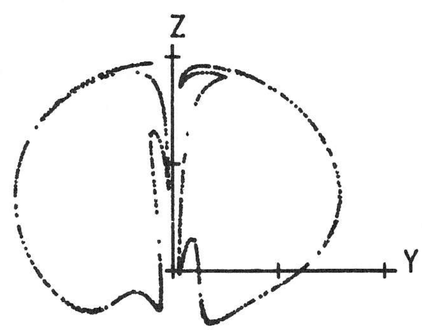

Fig. 10. 500 Poincaré Maps.

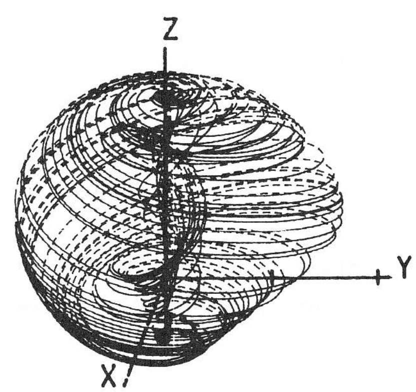

Fig. 11. Turbulence. Eps=0.25

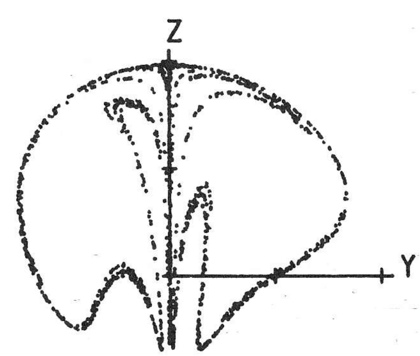

Fig. 12. 700 Poincaré Maps.

first glance, but rather an infinitely folded curve of infinite length, in fact a fractal object [22]. A blown up portion of an island in Figure 8 looks like a product of an interval with a Cantor set, see [21] for an analogous case.

Further increasing ε causes the chaotic bands to widen and appear to merge, eventually recreating the torus as in Figures 9 and 10, but now we have not a smooth manifold as in Figures 1 and 2, but a fractal object: a thick torus or bagel [23]. As ε increases further, the torus visibly thickens, and the flow becomes more and more "turbulent" or chaotic, see Figures 11 and 12. Still larger ε causes the attractor to contact its basin boundary, but it is not clear whether Newhouse sinks [24] are created in the process. The attractor bursts through its basin boundary, and due to the nonaxisymmetry this occurs at first in a very small region which a trajectory may fail to find for a long time. The result is "transient chaos", see Figure 13, with $\varepsilon = 0.28$. A typical trajectory now resembles the chaotic trajectory of Figure 11 for a long but finite time, but finally escapes from the chaotic region and is drawn to another attractor, in this case a stable node on the negative Z-axis. This stable node coexists with the torus and chaotic attractors above for smaller values of ε, and the boundary separating their basins of attraction can be extremely complicated, probably another fractal set. Another example of coexistence of attractors with complicated (fractal?) basin boundaries is shown in Figure 14, where $\varepsilon = 0.07$ and $\omega = 5$. Two limit cycles of periods 5 and 6, represented by the symbols X and O respectively, coexist within the "ghost" of the former invariant torus. Very small changes in initial points affect which cycle a trajectory eventually approaches, and in fact preliminary work indicates that the basin boundaries may be as complicated as the Julia sets of iterated mappings of the complex plane.

4. Conclusions

Numerical computations have shown evidence of phase locking, period doubling, coexistence of attractors, strange attractors varying from a chaotic band to a thick torus, and transient chaos, all resulting from nonaxisymmetric perturbations of an invariant torus. This provides new information on the unfoldings of the hysteresis-Hopf singularity. In addition these model equations may help in understanding the general problem of bifurcations from invariant tori in 3D flows. Considerable recent effort has gone into studies of bifurcations of maps of an interval [25], and of a plane [26]; much of the motivation for that work comes from Poincaré maps of flows, but flows themselves have been considered too expensive for direct study. The simple model equation (2) and those in [17,19] remove that obstacle, opening the way to detailed computer-assisted direct studies of the bifurcations from tori to strange attractors.

Figures 7 to 12 show only a few samples of the variety of phase portraits of chaotic or strange attractors for this system. It seems likely that these attractors are topologically inequivalent and thus not structurally stable in the classical sense. Yet in a practical sense they form a continuum, a small perturbation of one of these strange attractors yields a new strange attractor with similar qualitative behavior. This suggests that it may be necessary to devise a new more global definition of structural stability to deal with such strange attractors. The strange attractors studied here withstood perturbations far greater those that destroyed the invariant tori which gave rise to them. Thus the local existence of quasiperiodic tori proven in [18] may be very local indeed, while these strange attractors, whose existence has not yet been proven rigorously, may in fact persist more globally.

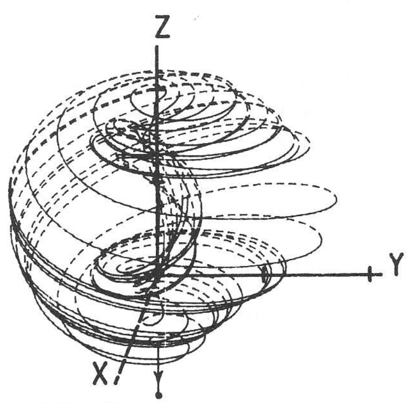

Fig. 13. Transient Chaos.

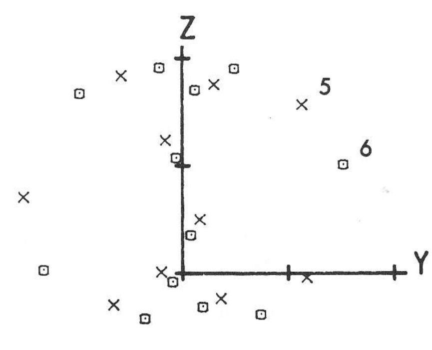

Fig. 14. Coexistence.

REFERENCES

[1] H.L. Swinney and J.P. Gollub. Hydrodynamic Instabilities and the Transition to Turbulence. Springer-Verlag, New York (1981).

[2] G. Iooss and D.D. Joseph. Nonlinear Dynamics and Turbulence, Pitman Press. To appear.

[3] R.E. Meyer. Transition and Turbulence. Academic Press, New York (1981).

[4] Proceedings of the International Conference on Order in Chaos, Los Alamos, NM. Physica D, V. 7D (1983) Nos. 1-3.

[5] R. Abraham and J.E. Marsden. Foundations of Mechanics, 2nd Ed. Benjamin/Cummings Reading MA (1978).

[6] G. Iooss and W.F. Langford. Conjectures on the Routes to Turbulence via Bifurcations. Ann. N.Y. Acad. Sci., V. 357 (1980) pp. 489-505.

[7] J.P. Gollub and S.V. Benson. Many routes to turbulent convection. J. Fluid Mech., V. 100 (1980) pp. 449-470.

[8] P.R. Fenstermacher, H.L. Swinney and J.P. Gollub. Dynamical instabilities and the transition to chaotic Taylor vortex flow. J. Fluid Mech., V. 94 (1979) 103-128.

[9] C. Vidal, J.-C. Roux, S. Bachelart and A. Rossi. Experimental study of the transition to turbulence in the Belousov-Zhabotinsky reaction. Ann. N.Y. Acad. Sci., V. 357 (1980) pp. 377-396.

[10] W.F. Langford. Periodic and steady-state mode interactions lead to tori. SIAM J. Appl. Math., V. 37 (1979) pp. 22-48.

[11] W.F. Langford and G. Iooss. Interactions of Hopf and pitchfork bifurcations. Bifurcation Problems and their Numerical Solution, H.D. Mittelmann and H. Weber (Eds). ISNM 54, Birkhauser Verlag, Basel (1980) pp. 103-134.

[12] J. Guckenheimer. On a codimension two bifurcation. Dynamical Systems and Turbulence, Warwick 1980, D.A. Rand and L.S. Young (Eds). Lecture Notes in Mathematics No. 898, Springer-Verlag, New York (1981) pp. 99-142.

[13] P.J. Holmes. Unfolding a degenerate nonlinear oscillator: a codimension two bifurcation. Ann. N.Y. Acad. Sci., V. 357 (1980) pp. 473-488.

[14] S.-N. Chow and J.K. Hale. Methods of Bifurcation Theory. Springer-Verlag, New York (1982).

[15] J. Guckenheimer and P. Holmes. Nonlinear Oscillations, Dynamical Systems, and Bifurcations of Vector Fields. Springer-Verlag, New York (1983).

[16] F. Spirig. Sequence of bifurcations in a three-dimensional system near a critical point. J. Appl. Math. Mech. (ZAMP) V. 34 (1983) pp. 259-276.

[17] W.F. Langford. A review of interactions of Hopf and steady-state bifurcations. To appear in [2].

[18] J. Scheurle and J. Marsden. Bifurcation to quasiperiodic tori in the interaction of steady-state and Hopf bifurcations. Preprint, Berkeley, Calif. (1982).

[19] W.F. Langford. Unfoldings of degenerate bifurcations. Dynamical Systems, Fractals and Chaos, P. Fischer and W.R. Smith (Eds), Marcel Dekker. To appear.

[20] W.F. Langford. Chaotic dynamics in the unfoldings of degenerate bifurcations. Proceedings of the International Symposium on Applied Mathematics and Information Science, Kyoto University, Japan (1982).

[21] J. Perreault. M.Sc. Thesis, Dept. of Mathematics, McGill University, Montreal (1983).

[22] B.B. Mandelbrot. The Fractal Geometry of Nature. W.H. Freeman, San Francisco (1983).

[23] R.H. Abraham and C.D. Shaw. Dynamics - The Geometry of Behaviour. Part 2: Chaotic Behaviour. Aerial Press, Santa Cruz (1983).

[24] S.E. Newhouse. The abundance of wild hyperbolic sets and nonsmooth stable sets for diffeomorphisms. Publ. Math. IHES, V. 50 (1979) pp. 101-151.

[25] P. Collet and J.-P. Eckmann. Iterated Maps on the Interval as Dynamical Systems. Prog. Phys. V. 1, Birkhauser Boston (1980).

[26] D.G. Aronson, M.A. Chory, G.R. Hall, and R.P. McGehee. Bifurcations from an invariant circle for two-parameter families of maps of the plane: a computer assisted study. Commun. Math. Phys., V. 83 (1982) pp. 303-354.

W.F. Langford
Department of Mathematics and Statistics
University of Guelph
Guelph, Ontario
Canada N1G 2W1